

# Hertz potentials approach to the dynamical Casimir effect in cylindrical cavities of arbitrary section

Martín Croce<sup>1</sup>, Diego A R Dalvit<sup>2</sup>, Fernando C Lombardo<sup>3</sup> and Francisco D Mazzitelli<sup>3</sup>

<sup>1</sup> Physics Department, New York University, 4 Washington Place, New York, NY 10003, USA

<sup>2</sup> Theoretical Division, MS B213 Los Alamos National Laboratory, Los Alamos, NM 87545, USA

<sup>3</sup> Departamento de Física Juan José Giambiagi, FCEyN UBA, Facultad de Ciencias Exactas y Naturales, Ciudad Universitaria, Pabellón I, 1428 Buenos Aires, Argentina

Received 2 September 2004, accepted for publication 23 November 2004

Published 1 March 2005

Online at [stacks.iop.org/JOptB/7/S32](http://stacks.iop.org/JOptB/7/S32)

## Abstract

We study the creation of photons in resonant cylindrical cavities with time-dependent length. The physical degrees of freedom of the electromagnetic field are described using Hertz potentials. We describe the general formalism for cavities with arbitrary section. Then we compute explicitly the number of TE and TM motion-induced photons for cylindrical cavities with rectangular and circular sections. We also discuss the creation of TEM photons in non-simply connected cylindrical cavities.

**Keywords:** cavity QED, Casimir effect, resonant photon creation

## 1. Introduction

In quantum field theory time-dependent boundary conditions or time-dependent background fields may induce particle creation, even when the initial state of a quantum field is the vacuum [1]. In the context of quantum electrodynamics, uncharged mirrors in accelerated motion can in principle create photons. This effect is referred to in the literature as the dynamical Casimir effect, or motion-induced radiation [2]. In particular, when the length of a high  $Q$  electromagnetic cavity oscillates with one of its resonant frequencies, the number of photons inside the cavity accumulates slowly and grows exponentially with time. Many authors have considered this problem using different approximations: from toy models of scalar fields in  $1 + 1$  dimensions [3] to the more realistic case of scalar [4, 5] and electromagnetic [6] fields in three-dimensional rectangular cavities. Arbitrary periodic motion of the boundary of an ideal cavity has been studied in [7]. The relevance of finite temperature effects and losses have also been considered [8].

Unlike the static Casimir effect [9], that has been measured with increasing precision in the last years [10], an experimental verification of the dynamical counterpart is still lacking.

The main reason is that typical resonance frequencies for microwave cavities are of the order of gigahertz. It is very difficult (although not impossible) to make a mirror oscillate at such frequencies. One possibility is to consider a two-dimensional array of nanoresonators coherently driven to oscillate at very high frequencies [11].

Several alternative proposals have been investigated in which the physical properties of the medium inside the cavity change with time, but with the boundary of the cavity kept fixed. For example, it has been proposed [12] that one could change effectively the length of a cavity by irradiating with ultra-short laser pulses a thin semiconductor film deposited on one of the walls of the cavity (see also [13]). Nonlinear optics may be used to produce effective fast moving mirrors.

From an experimental point of view, the idea of changing the effective length of a cavity by irradiating a semiconductor is promising [14]. A relevant possibility is to force periodic oscillations of the conductivity of the semiconductor, as this will enhance particle production for certain resonance frequencies [15]. The first estimations of the number of photons created in resonant situations are within the limits of the minimum signal that could be detected. It is then of interest to refine the calculations and to explore other

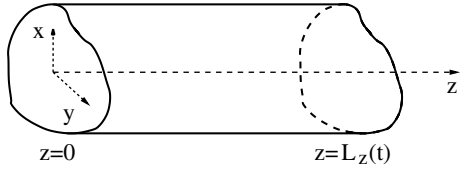


**Figure 1.** Hollow, cylindrical cavity of arbitrary cross-sectional shape.

geometries that could be relevant from an experimental point of view. In order to understand the effect of the geometry, in this paper we will analyse the moving mirror case for cylindrical cavities of arbitrary section (see figure 1). The physical degrees of freedom of the electromagnetic field will be expressed in terms of the so-called scalar Hertz potentials. We will reobtain previous results for rectangular cavities, and we will extend them to the case of cylindrical cavities with circular section. We will also consider the case of non-simply connected cylindrical cavities, since in this case one has additional transverse electromagnetic (TEM) modes.

The paper is organized as follows. In section 2 we introduce the Hertz potentials and we express the boundary conditions for moving mirrors in terms of them. We also show the equivalence of the description with previous approaches based on dual transverse electric (TE) and magnetic (TM) vector potentials. In section 3 we quantize the theory, and we find the relation between the number of TE and TM created photons with the number of particles associated with the scalar Hertz potentials. Section 4 includes explicit calculations for cavities with rectangular and circular sections. The case of coaxial resonant cavities is considered in section 5, where we quantize the TEM modes and show that they can be described by a one-dimensional scalar field. Section 6 contains a summary and a discussion of the results.

## 2. Classical description

### 2.1. Vector and scalar Hertz potentials

We consider in this section the representation of the physical degrees of freedom of the electromagnetic field in terms of Hertz potentials, which allows an alternative picture to the standard vector  $\mathbf{A}$  and scalar potentials  $\Phi$ . In the Lorentz gauge  $\mu\epsilon\partial_t\Phi + \nabla \cdot \mathbf{A} = 0$ , the Maxwell equations for linear media read

$$\mu\epsilon\frac{\partial^2\Phi}{\partial t^2} - \nabla^2\Phi = \frac{1}{\epsilon}\rho - \frac{1}{\epsilon}\nabla \cdot \mathbf{P}_0, \quad (1)$$

$$\mu\epsilon\frac{\partial^2\mathbf{A}}{\partial t^2} - \nabla^2\mathbf{A} = \mu\mathbf{J} + \mu\frac{\partial\mathbf{P}_0}{\partial t} + \nabla \times \mathbf{M}_0, \quad (2)$$

where we have included, in addition to the induced electric and magnetic polarizations (which are taken into account by the constants  $\epsilon$  and  $\mu$ ), permanent polarizations and magnetization  $\mathbf{P}_0$  and  $\mathbf{M}_0$ . These are introduced to motivate the form of the Hertz potentials [16, 17]. We are using SI units with  $\epsilon_0 = 1$ ,  $\mu_0 = 1$  and  $c = 1$ .

Now we introduce two vector potentials,  $\mathbf{\Pi}_e$  and  $\mathbf{\Pi}_m$ , by expressing  $\Phi$  and  $\mathbf{A}$  in a symmetric form with respect to the terms containing  $\mathbf{P}_0$  and  $\mathbf{M}_0$  in the rhs of equations (1), (2):

$$\Phi = -\frac{1}{\epsilon}\nabla \cdot \mathbf{\Pi}_e, \quad (3)$$

$$\mathbf{A} = \mu\frac{\partial\mathbf{\Pi}_e}{\partial t} + \nabla \times \mathbf{\Pi}_m. \quad (4)$$

$\mathbf{\Pi}_e$  and  $\mathbf{\Pi}_m$  are known as the electric and magnetic vector Hertz potentials [16, 18]. The equations satisfied by these potentials are simplified if one introduces two functions,  $\mathbf{Q}_e$  and  $\mathbf{Q}_m$ , known as stream potentials, as follows:

$$\rho = -\nabla \cdot \mathbf{Q}_e, \quad \mathbf{J} = \frac{\partial\mathbf{Q}_e}{\partial t} + \frac{1}{\mu}\nabla \times \mathbf{Q}_m. \quad (5)$$

Using equations (3)–(5) in equations (1), (2) one finally arrives at

$$(\mu\epsilon\partial_t^2 - \nabla^2)\mathbf{\Pi}_e = \mathbf{Q}_e + \mathbf{P}_0, \quad (6)$$

$$(\mu\epsilon\partial_t^2 - \nabla^2)\mathbf{\Pi}_m = \mathbf{Q}_m + \mathbf{M}_0. \quad (7)$$

There is a gauge freedom that must be suitably fixed in order to obtain equations (6) and (7) [18]. The electric field and magnetic induction are given in terms of the vector Hertz potentials by

$$\mathbf{E} = \frac{1}{\epsilon}\nabla(\nabla \cdot \mathbf{\Pi}_e) - \mu\frac{\partial^2\mathbf{\Pi}_e}{\partial t^2} - \nabla \times \frac{\partial\mathbf{\Pi}_m}{\partial t}, \quad (8)$$

$$\mathbf{B} = \mu\nabla \times \frac{\partial\mathbf{\Pi}_e}{\partial t} + \nabla \times (\nabla \times \mathbf{\Pi}_m). \quad (9)$$

In vacuum at points away from the sources, the fields can be expressed in terms of only two scalar functions, the so-called scalar Hertz potentials, each satisfying a homogeneous wave equation [16]. This result translates to the Hertz formalism by writing

$$\mathbf{\Pi}_e = \phi\hat{\mathbf{e}}_3, \quad \mathbf{\Pi}_m = \psi\hat{\mathbf{e}}_3, \quad (10)$$

where  $\hat{\mathbf{e}}_3$  is a unit vector in a fixed direction. In this way  $\psi$  gives rise to TE fields with respect to  $\hat{\mathbf{e}}_3$ , whereas  $\phi$  represents TM fields. For our purposes  $\hat{\mathbf{e}}_3$  will be taken along the longitudinal axis of the cylindrical cavity. Moreover we will use either Cartesian or cylindrical coordinates in this paper, with  $\hat{\mathbf{e}}_3 = \hat{\mathbf{z}}$  in both cases. The transverse directions ( $\hat{\mathbf{e}}_1, \hat{\mathbf{e}}_2$ ) will stand for  $(\hat{\mathbf{x}}, \hat{\mathbf{y}})$  in the first case and  $(\hat{\rho}, \hat{\phi})$  in the second.

The potentials and fields can be written in terms of the two scalar Hertz potentials using equation (10) in equations (3), (4), (8), (9). The result is

$$\Phi = -\partial_z\phi, \quad (11)$$

$$\mathbf{A} = \partial_2\psi\hat{\mathbf{e}}_1 - \partial_1\psi\hat{\mathbf{e}}_2 + \partial_t\phi\hat{\mathbf{z}}, \quad (12)$$

$$\mathbf{E} = (\partial_1\partial_z\phi - \partial_2\partial_t\psi)\hat{\mathbf{e}}_1 + (\partial_2\partial_z\phi + \partial_1\partial_t\psi)\hat{\mathbf{e}}_2 - (\nabla_\perp^2\phi)\hat{\mathbf{z}}, \quad (13)$$

$$\mathbf{B} = (\partial_2\partial_t\phi + \partial_1\partial_z\psi)\hat{\mathbf{e}}_1 + (-\partial_1\partial_t\phi + \partial_2\partial_z\psi)\hat{\mathbf{e}}_2 - (\nabla_\perp^2\psi)\hat{\mathbf{z}}, \quad (14)$$

where the transverse Laplacian is defined as  $\nabla_\perp^2 \equiv \nabla^2 - \frac{\partial^2}{\partial z^2}$ . In Cartesian coordinates  $(\partial_1, \partial_2) = (\frac{\partial}{\partial x}, \frac{\partial}{\partial y})$  and  $\nabla_\perp^2 = \frac{\partial^2}{\partial x^2} + \frac{\partial^2}{\partial y^2}$ . In cylindrical coordinates  $(\partial_1, \partial_2) = (\frac{\partial}{\partial \rho}, \frac{1}{\rho}\frac{\partial}{\partial \phi})$  and  $\nabla_\perp^2 = \frac{1}{\rho}\frac{\partial}{\partial \rho}(\frac{1}{\rho}\frac{\partial}{\partial \rho}) + \frac{1}{\rho^2}\frac{\partial^2}{\partial \phi^2}$ .

In previous works [6, 19], the electromagnetic degrees of freedom have been described in terms of two vector potentials  $\mathbf{A}_{TE}$  and  $\mathbf{A}_{TM}$  with null divergence and  $\mathbf{z}$ -component. The TE electric and magnetic fields are given by

$$\mathbf{E}_{TE} = -\dot{\mathbf{A}}_{TE}, \quad \mathbf{B}_{TE} = \nabla \times \mathbf{A}_{TE}, \quad (15)$$

while the TM fields are given by the dual relations

$$\mathbf{B}_{\text{TM}} = \dot{\mathbf{A}}_{\text{TM}}, \quad \mathbf{E}_{\text{TM}} = \nabla \times \mathbf{A}_{\text{TM}}. \quad (16)$$

Comparing equations (15) and (16) with the expressions for the electromagnetic fields in terms of the Hertz potentials equations (8)–(10), we obtain

$$\begin{aligned} \mathbf{A}_{\text{TE}} &= \nabla \times \mathbf{\Pi}_m = \hat{\mathbf{z}} \times \nabla \psi, \\ \mathbf{A}_{\text{TM}} &= \nabla \times \mathbf{\Pi}_e = \hat{\mathbf{z}} \times \nabla \phi, \end{aligned} \quad (17)$$

so both approaches are equivalent.

The description in terms of independent TE and TM fields is possible due to the particular geometries we are considering. Indeed, using the above definitions and boundary conditions (see below) it is easy to check that no mixed terms appear in Maxwell's Lagrangian and Hamiltonian.

### 2.2. Boundary conditions for a perfect conducting cavity

In the static case, the boundary conditions for the fields over the walls of the cavity are  $\mathbf{E}_t = 0$  and  $\mathbf{B}_n = 0$ . These translate into conditions for the two scalar potentials through equations (13), (14). The scalar Hertz potential  $\psi$  satisfies Dirichlet boundary conditions on the longitudinal boundary ( $z = 0, L_z$ ) and Neumann boundary conditions on the transverse boundaries,

$$\psi|_{z=0, L_z} = 0, \quad \left. \frac{\partial \psi}{\partial n} \right|_{\text{trans}} = 0. \quad (18)$$

On the other hand, the scalar Hertz potential  $\phi$  satisfies Neumann boundary conditions on the longitudinal boundary ( $z = 0, L_z$ ) and Dirichlet boundary conditions on the transverse boundaries,

$$\left. \frac{\partial \phi}{\partial z} \right|_{z=0, L_z} = 0, \quad \phi|_{\text{trans}} = 0. \quad (19)$$

Let us now consider the boundary conditions in the case when one of the surfaces is moving, say  $z = L_z(t)$ . The boundary conditions on a moving interface between two media containing a surface charge density  $\sigma$  and a surface current  $\mathbf{K}$  are [20]

$$\begin{aligned} (\mathbf{D}_{\text{II}} - \mathbf{D}_{\text{I}}) \cdot \mathbf{n} &= \sigma, \\ (\mathbf{B}_{\text{II}} - \mathbf{B}_{\text{I}}) \cdot \mathbf{n} &= 0, \\ [\mathbf{n} \times (\mathbf{H}_{\text{II}} - \mathbf{H}_{\text{I}}) + (\mathbf{v} \cdot \mathbf{n})(\mathbf{D}_{\text{II}} - \mathbf{D}_{\text{I}})] \cdot \mathbf{t} &= \mathbf{K} \cdot \mathbf{t}, \\ [\mathbf{n} \times (\mathbf{E}_{\text{II}} - \mathbf{E}_{\text{I}}) - (\mathbf{v} \cdot \mathbf{n})(\mathbf{B}_{\text{II}} - \mathbf{B}_{\text{I}})] \cdot \mathbf{t} &= 0, \end{aligned} \quad (20)$$

where  $\mathbf{n}$  denotes the normal to the interface going from medium I to medium II, and  $\mathbf{t}$  is any unit vector tangential to the surface. These conditions can be derived by performing a Lorentz transformation to the reference system where the surface is instantaneously at rest [19], or by consistency of the Maxwell equations in the laboratory frame [20].

We assume the moving wall to be a perfect conductor. Therefore the fields vanish exactly in region II and the boundary conditions in equation (20) become

$$\mathbf{B} \cdot \hat{\mathbf{z}} = 0, \quad (\mathbf{E} \times \hat{\mathbf{z}} + v\mathbf{B}) \cdot \mathbf{t} = 0, \quad (21)$$

where  $v = \dot{L}_z$ . In terms of the two scalar Hertz potentials we obtain

$$\psi(z = L_z(t)) = 0, \quad (\partial_z + v \partial_0)\phi(z = L_z(t)) = 0, \quad (22)$$

that modify the boundary conditions in equations (18) and (19) on the moving longitudinal boundary ( $z = L_z(t)$ ).

## 3. Quantum description

In this section we will quantize the electromagnetic field using the scalar Hertz potentials formalism. We will also obtain the relation between the Bogoliubov coefficients relating IN and OUT bases of the scalar field with those of the electromagnetic field. We will assume that the cavity is at rest for  $t < 0$ , and that the wall placed at  $z = L_z$  begins to move with a prescribed trajectory  $L_z(t)$ . We will mainly concentrate on harmonic motions of the type

$$L_z(t) = L_0 [1 + \epsilon \sin \Omega t + \epsilon f(t)], \quad (23)$$

where  $f(t)$  is some decaying function that allows us to meet the continuity conditions at  $t = 0$ . The motion ends at  $t = T$ .

### 3.1. Transverse electric scalar field

Let us start with the TE scalar Hertz potential  $\psi$ . We expand the field as

$$\psi(\mathbf{x}, t) = \sum_{\mathbf{k}} C_{\mathbf{k}} a_{\mathbf{k}}^{\text{IN}} u_{\mathbf{k}, \text{TE}}^{\text{IN}}(\mathbf{x}, t) + \text{h.c.}, \quad (24)$$

where  $u_{\mathbf{k}, \text{TE}}^{\text{IN}}(\mathbf{x}, t)$  are the solutions of the Klein–Gordon equation which have positive frequency in the IN region ( $t < 0$ ),  $a_{\mathbf{k}}^{\text{IN}}$  are the corresponding annihilation bosonic operators, and  $C_{\mathbf{k}}$  are normalization constants. The summation index is  $\mathbf{k} = (\mathbf{k}_{\perp}, k_z = n_z \pi / L_z)$ . In the IN region the explicit form of the solution is

$$u_{\mathbf{k}, \text{TE}}^{\text{IN}}(\mathbf{x}, t) = \frac{e^{-i\omega_{\mathbf{k}} t}}{\sqrt{2\omega_{\mathbf{k}}}} \sqrt{\frac{2}{L_z}} \sin(k_z z) v_{\mathbf{k}_{\perp}}(\mathbf{x}_{\perp}), \quad (25)$$

with  $\nabla_{\perp}^2 v_{\mathbf{k}_{\perp}} = -\mathbf{k}_{\perp}^2 v_{\mathbf{k}_{\perp}}$  and  $\omega_{\mathbf{k}} = |\mathbf{k}|$ . The set of functions  $v_{\mathbf{k}_{\perp}}$  satisfies Neumann boundary conditions on the lateral surface and can be assumed to be real and orthonormal on the plane  $\mathbf{x}_{\perp}$ .

In order to fix the normalization constants  $C_{\mathbf{k}}$  and the commutation relations between creation and annihilation operators, we compute the Hamiltonian of the electromagnetic field. We find

$$\begin{aligned} H &= \frac{1}{8\pi} \int d^3x (\mathbf{E}^2 + \mathbf{B}^2) \\ &= \frac{1}{8\pi} \int d^3x (-\psi \nabla_{\perp}^2 \psi + \nabla^2 \psi \nabla_{\perp}^2 \psi) \\ &= \sum_{\mathbf{k}} \frac{|C_{\mathbf{k}}|^2}{8\pi} \mathbf{k}_{\perp}^2 \omega_{\mathbf{k}} (a_{\mathbf{k}}^{\text{IN}} (a_{\mathbf{k}}^{\text{IN}})^{\dagger} + \text{h.c.}). \end{aligned} \quad (26)$$

Therefore, with the choice  $|C_{\mathbf{k}}| = \sqrt{8\pi}/|\mathbf{k}_{\perp}|$ , the operators  $a_{\mathbf{k}}^{\text{IN}}$  and  $(a_{\mathbf{k}}^{\text{IN}})^{\dagger}$  satisfy the usual commutation relations [17].

For  $0 < t < T$  we expand the IN basis in an instantaneous basis

$$u_{\mathbf{k},\text{TE}}^{\text{IN}} = \sum_{\mathbf{p}} Q_{\mathbf{p},\text{TE}}^{(\mathbf{k})}(t) \sqrt{\frac{2}{L_z(t)}} \sin(p_z(t)z) v_{\mathbf{p}_\perp}(\mathbf{x}_\perp), \quad (27)$$

where  $p_z(t) = p_z \pi / L_z(t)$ . The initial conditions are

$$Q_{\mathbf{p},\text{TE}}^{(\mathbf{k})}(0) = \frac{1}{\sqrt{2\omega_{\mathbf{k}}}} \delta_{\mathbf{p}\mathbf{k}}, \quad \dot{Q}_{\mathbf{p},\text{TE}}^{(\mathbf{k})}(0) = -i\sqrt{\frac{\omega_{\mathbf{k}}}{2}} \delta_{\mathbf{p}\mathbf{k}}. \quad (28)$$

This expansion must be a solution of the wave equation. Using the fact that both  $\sin(p_z(t)z)$  and  $v_{\mathbf{p}_\perp}(\mathbf{x}_\perp)$  form a complete and orthonormal set, and the fact that they only depend on  $t$  through  $L_z(t)$ , we obtain a set of coupled equations for the temporal coefficients  $Q_{\mathbf{p},\text{TE}}^{(\mathbf{k})}(t)$  [6]

$$\ddot{Q}_{\mathbf{p},\text{TE}}^{(\mathbf{k})} + \omega_{\mathbf{p}}^2(t) Q_{\mathbf{p},\text{TE}}^{(\mathbf{k})} = 2\lambda(t) \sum_{\mathbf{j}} g_{\mathbf{p}\mathbf{j}} \dot{Q}_{\mathbf{j},\text{TE}}^{(\mathbf{k})} + \dot{\lambda}(t) \sum_{\mathbf{j}} g_{\mathbf{p}\mathbf{j}} Q_{\mathbf{j},\text{TE}}^{(\mathbf{k})} + \text{O}(\epsilon^2), \quad (29)$$

where

$$\omega_{\mathbf{p}}(t) = \sqrt{\mathbf{p}_\perp^2 + \left(\frac{p_z \pi}{L_z(t)}\right)^2}, \quad \lambda(t) = \frac{\dot{L}_z(t)}{L_z(t)}. \quad (30)$$

The coupling coefficients are given by

$$g_{\mathbf{p}\mathbf{j}} = -g_{\mathbf{j}\mathbf{p}} = \begin{cases} (-1)^{p_z+j_z} \frac{2p_z j_z}{j_z^2 - p_z^2} \delta_{\mathbf{p}_\perp, \mathbf{j}_\perp} & \text{if } p_z \neq j_z \\ 0 & \text{if } p_z = j_z. \end{cases} \quad (31)$$

For  $t > T$  (OUT region), the time-dependent coefficients  $Q_{\mathbf{p},\text{TE}}^{\mathbf{k}}$  become

$$Q_{\mathbf{p},\text{TE}}^{\mathbf{k}} = A_{\mathbf{p},\text{TE}}^{\mathbf{k}} \frac{e^{-i\omega_{\mathbf{k}} t}}{\sqrt{2\omega_{\mathbf{k}}}} + B_{\mathbf{p},\text{TE}}^{\mathbf{k}} \frac{e^{i\omega_{\mathbf{k}} t}}{\sqrt{2\omega_{\mathbf{k}}}}. \quad (32)$$

We introduce the OUT basis  $u_{\mathbf{k},\text{TE}}^{\text{OUT}}(\mathbf{x}, t)$  as the set of solutions of the Klein–Gordon equation that are of the form given in the rhs of equation (25) in the OUT region. The IN and OUT bases are then related by the Bogoliubov transformation:

$$u_{\mathbf{k},\text{TE}}^{\text{IN}} = \sum_{\mathbf{p}} B_{\mathbf{p},\text{TE}}^{\mathbf{k}} (u_{\mathbf{p},\text{TE}}^{\text{OUT}})^* + A_{\mathbf{p},\text{TE}}^{\mathbf{k}} u_{\mathbf{p},\text{TE}}^{\text{OUT}}. \quad (33)$$

Using this relation it is easy to show that the number of OUT photons with TE polarization and wavevector  $\mathbf{k}$  is given by

$$\langle N_{\mathbf{k},\text{TE}} \rangle = \langle 0_{\text{IN}} | (a_{\mathbf{k}}^{\text{OUT}})^\dagger a_{\mathbf{k}}^{\text{OUT}} | 0_{\text{IN}} \rangle = \mathbf{k}_\perp^2 \sum_{\mathbf{p}} \frac{|B_{\mathbf{k},\text{TE}}^{\mathbf{p}}|^2}{\mathbf{p}_\perp^2}. \quad (34)$$

### 3.2. Transverse magnetic scalar field

The quantization of the TM scalar Hertz potential  $\phi$  is analogous to that of  $\psi$ . The explicit form for the IN basis is now given by

$$u_{\mathbf{k},\text{TM}}^{\text{IN}}(\mathbf{x}, t) = \frac{e^{-i\omega_{\mathbf{k}} t}}{\sqrt{2\omega_{\mathbf{k}}}} \sqrt{\frac{2}{L_z}} \cos(k_z z) r_{\mathbf{k}_\perp}(\mathbf{x}_\perp), \quad (35)$$

with  $\nabla_\perp^2 r_{\mathbf{k}_\perp} = -\mathbf{k}_\perp^2 r_{\mathbf{k}_\perp}$ , the functions  $r_{\mathbf{k}_\perp}$  satisfying Dirichlet boundary conditions on the lateral surface. Following [6], we introduce the instantaneous basis

$$u_{\mathbf{k},\text{TM}}^{\text{IN}} = \sum_{\mathbf{p}} (Q_{\mathbf{p},\text{TM}}^{(\mathbf{k})}(t) + \dot{Q}_{\mathbf{p},\text{TM}}^{(\mathbf{k})}(t) g(z, t)) \times \sqrt{\frac{2}{L_z(t)}} \cos(p_z(t)z) r_{\mathbf{k}_\perp}(\mathbf{x}_\perp). \quad (36)$$

The initial conditions for  $Q_{\mathbf{p},\text{TM}}^{(\mathbf{k})}$  are the same as those for  $Q_{\mathbf{p},\text{TE}}^{(\mathbf{k})}$ . The function  $g(z, t)$  can be expressed as  $g(z, t) = \dot{L}_z(t) L_z(t) \xi(z/L_z(t))$ , where  $\xi(z)$  is a solution to the conditions  $\xi(0) = \xi(1) = 0$ ,  $\partial_z \xi(0) = 0$ , and  $\partial_z \xi(1) = -1$  [6]. There are many solutions to these conditions, implying a freedom for selecting the instantaneous basis. However, it can be proved that physical quantities, such as the mean number of created TM photons or the energy density inside the cavity, are independent of the particular choice of  $g(z, t)$  [6]. The equation of motion for  $Q_{\mathbf{p},\text{TM}}^{(\mathbf{k})}$  is similar to equation (29) for  $Q_{\mathbf{p},\text{TE}}^{(\mathbf{k})}$ , namely

$$\begin{aligned} \ddot{Q}_{\mathbf{p},\text{TM}}^{(\mathbf{k})} + \omega_{\mathbf{k}}^2(t) Q_{\mathbf{p},\text{TM}}^{(\mathbf{k})} &= -2\lambda(t) \sum_{\mathbf{j}} h_{\mathbf{j}\mathbf{p}} \dot{Q}_{\mathbf{p},\text{TM}}^{(\mathbf{k})} - \dot{\lambda}(t) \sum_{\mathbf{j}} h_{\mathbf{j}\mathbf{p}} Q_{\mathbf{p},\text{TM}}^{(\mathbf{k})} \\ &\quad - 2\dot{\lambda}(t) L_z^2(t) \sum_{\mathbf{j}} s_{\mathbf{j}\mathbf{p}} \ddot{Q}_{\mathbf{p},\text{TM}}^{(\mathbf{k})} \\ &\quad - \sum_{\mathbf{j}} \dot{Q}_{\mathbf{p},\text{TM}}^{(\mathbf{k})} [s_{\mathbf{j}\mathbf{p}} \ddot{\lambda}(t) L_z^2(t) - \lambda(t) \eta_{\mathbf{j}\mathbf{p}}] \\ &\quad - \lambda(t) L_z^2(t) \sum_{\mathbf{j}} s_{\mathbf{j}\mathbf{p}} \partial_t^3 Q_{\mathbf{p},\text{TM}}^{(\mathbf{k})} + \text{O}(\epsilon^2), \end{aligned} \quad (37)$$

where the coefficients  $s_{\mathbf{j}\mathbf{p}}$ ,  $\eta_{\mathbf{j}\mathbf{p}}$  and  $h_{\mathbf{j}\mathbf{p}}$  are given by

$$\begin{aligned} s_{\mathbf{j}\mathbf{p}} &= \int_0^{L_z(t)} dz \xi(z) \chi_{\mathbf{j}} \chi_{\mathbf{p}}, \\ \eta_{\mathbf{j}\mathbf{p}} &= L_z^2(t) \int_0^{L_z(t)} dz [(\xi''(z) - \omega_{\mathbf{j}}^2 \xi(z)) \chi_{\mathbf{j}} \chi_{\mathbf{k}} + 2\xi'(z) \chi_{\mathbf{j}}' \chi_{\mathbf{k}}], \\ h_{\mathbf{j}\mathbf{p}} &= \begin{cases} (-1)^{p_z+j_z} \frac{2j_z^2}{p_z^2 - j_z^2} \delta_{\mathbf{p}_\perp, \mathbf{j}_\perp} & \text{if } p_z \neq j_z \\ -\delta_{\mathbf{p}_\perp, \mathbf{j}_\perp} & \text{if } p_z = j_z. \end{cases} \end{aligned}$$

Here ' denotes derivative with respect to  $z$ . The functions  $\chi_{\mathbf{j}} \equiv \sqrt{2/L_z(t)} \sin(n_z \pi z / L_z(t))$  are normalized in the interval  $[0, L_z(t)]$ . Note that the above coefficients are independent of the particular form of the spatial modes  $r_{\mathbf{j}_\perp}(\mathbf{x}_\perp)$  for the transversal section.

The equation for the number of TM photons in the OUT region is similar to equation (34), with  $B_{\mathbf{k},\text{TE}}^{\mathbf{p}}$  replaced by  $B_{\mathbf{k},\text{TM}}^{\mathbf{p}}$ . Equation (34) and its TM counterpart are very useful because they relate the number of motion-induced photons with the Bogoliubov transformation of two scalar fields. Therefore, the analysis is simplified since it does not involve any reference to the polarization of the electromagnetic field. Moreover, the information about the transversal section of the cavity only enters through the spectrum  $\omega_{\mathbf{k}}$ .

## 4. Applications

In this section we will compute the number of photons created in resonant situations, for cylindrical cavities with either

rectangular or circular sections. The equations of motion for the coefficients  $Q_{\mathbf{p},\text{TE}}^{(\mathbf{k})}$  of the scalar Hertz potential  $\Psi$  (equation (29)) and the similar one for the scalar Hertz potential  $\phi$  (equation (37)) describe a set of coupled harmonic oscillators with periodic frequencies and couplings. They are of the same form as the equations that describe the modes of a scalar field in a three-dimensional cavity with an oscillating boundary, and can be solved using multiple scale analysis (MSA). For a detailed description of the method see, for example, [4].

In the ‘parametric resonant case’, in which the external frequency  $\Omega$  is twice the frequency of an unperturbed mode  $\mathbf{k}$  ( $\Omega = 2\omega_{\mathbf{k}}$ ), equations (29) and (37) lead to a resonant behaviour of the solutions. Moreover, there is intermode coupling between modes  $\mathbf{j}$  and  $\mathbf{k}$  if any of the resonant coupling conditions  $\Omega = |\omega_{\mathbf{k}} \pm \omega_{\mathbf{j}}|$  is satisfied. This is the case, for example, for 1D geometries and cubic cavities. Except for special geometries, in general the resonant coupling conditions are not met: different  $\mathbf{k}$  modes will not be coupled during the dynamics, and equations (29) and (37) reduce to the Mathieu equation for a single mode. In consequence, the number of motion-induced photons in that given mode will grow exponentially. The growth rate is different for TE and TM modes. This is due to the fact that, while the rhs of equation (29) vanishes for  $\mathbf{j} = \mathbf{p}$ , this is not the case in equation (37). The result is

$$\langle N_{\mathbf{k},\text{TE}}(t) \rangle = \sinh^2(\lambda_{\mathbf{k},\text{TE}}\epsilon t), \quad (38)$$

$$\langle N_{\mathbf{k},\text{TM}}(t) \rangle = \sinh^2(\lambda_{\mathbf{k},\text{TM}}\epsilon t), \quad (39)$$

where  $\lambda_{\mathbf{k},\text{TE}} = k_z^2/2\omega_{\mathbf{k}}$  and  $\lambda_{\mathbf{k},\text{TM}} = (2\omega_{\mathbf{k}}^2 - k_z^2)/2\omega_{\mathbf{k}}$ . Note that when both polarizations are present, the rate of growth for TM photons is larger than for TE photons, i.e.,  $\lambda_{\mathbf{k},\text{TM}} > \lambda_{\mathbf{k},\text{TE}}$ . As already mentioned, these expressions are independent of the mode functions in the transverse direction,  $v_{\mathbf{k}_{\perp}}(\mathbf{x}_{\perp})$  or  $r_{\mathbf{k}_{\perp}}(\mathbf{x}_{\perp})$ . The dependence on the sectional geometry enters only through the spectrum  $\omega_{\mathbf{k}}$ . The above expressions for the growth rates equations (38), (39) are valid for uncoupled modes. When there is mode coupling, the expressions for the growth rates are different, as explained in [4, 6].

#### 4.1. Cavities with rectangular section

This problem has been analysed previously in [6]. The transverse mode functions  $v_{\mathbf{k}_{\perp}}(\mathbf{x}_{\perp})$  associated with the scalar Hertz potential  $\psi$  are

$$v_{n_x, n_y}(\mathbf{x}_{\perp}) = \frac{2}{\sqrt{L_x L_y}} \cos\left(\frac{n_x \pi x}{L_x}\right) \cos\left(\frac{n_y \pi y}{L_y}\right), \quad (40)$$

where  $n_x$  and  $n_y$  are non-negative integers that cannot be simultaneously zero. The spectrum is ( $n_z \geq 1$ )

$$\omega_{n_x, n_y, n_z} = \sqrt{(n_x \pi/L_x)^2 + (n_y \pi/L_y)^2 + (n_z \pi/L_z)^2}. \quad (41)$$

The transverse mode functions  $r_{\mathbf{k}_{\perp}}(\mathbf{x}_{\perp})$  associated with the scalar Hertz potential  $\phi$  are

$$r_{m_x, m_y}(\mathbf{x}_{\perp}) = \frac{2}{\sqrt{L_x L_y}} \sin\left(\frac{m_x \pi x}{L_x}\right) \sin\left(\frac{m_y \pi y}{L_y}\right), \quad (42)$$

where  $m_x$  and  $m_y$  are integers, such that  $m_x, m_y \geq 1$ . The spectrum is given by equation (41) with  $n_z \geq 0$ .

As an example, we consider the parametric resonant case  $\Omega = 2\omega_{\mathbf{k}}$ , and show the results for the number of photons created in a cubic cavity of size  $L$ . Let us denote the modes by  $(n_x, n_y, n_z)$ . For the TE case, the fundamental mode is doubly degenerate ((1, 0, 1) and (0, 1, 1)) and uncoupled to other higher modes. The number of TE photons in these modes grows exponentially as  $\exp(\pi\epsilon t/\sqrt{2}L)$ . The fundamental mode for the TM fields corresponds to (1, 1, 0), and is coupled to the mode (1, 1, 4). The number of TM photons in these modes grows as  $\exp(4.4\epsilon t/L)$  [6]. The lowest possible excitable frequency of the field equals the fundamental frequency of both the TE and TM spectra. However, the exponential growth of motion-induced TM photons with fundamental energy in greater than that of TE photons.

#### 4.2. Cavities with circular section

Let us now introduce cylindrical coordinates  $(\rho, \phi, z)$  to consider a cylinder with circular section of radius  $\rho = R$ . The transverse mode functions  $v_{\mathbf{k}_{\perp}}(\mathbf{x}_{\perp})$  related to TE fields are

$$v_{nm}(\mathbf{x}_{\perp}) = \frac{1}{\sqrt{\pi}} \frac{1}{R J_n(y_{nm}) \sqrt{1 - n^2/y_{nm}^2}} J_n\left(y_{nm} \frac{\rho}{R}\right) e^{in\phi}, \quad (43)$$

where  $J_n$  denotes the Bessel function of  $n$ th order, and  $y_{nm}$  is the  $m$ th positive root of the equation  $J_n'(y) = 0$ . The eigenfrequencies are given by ( $n_z \geq 1$ )

$$\omega_{n, m, n_z} = \sqrt{\left(\frac{y_{nm}}{R}\right)^2 + \left(\frac{n_z \pi}{L_z}\right)^2}. \quad (44)$$

The solution for the mode functions  $r_{\mathbf{k}_{\perp}}(\mathbf{x}_{\perp})$  associated with TM fields is

$$r_{nm}(\mathbf{x}_{\perp}) = \frac{1}{\sqrt{\pi}} \frac{1}{R J_{n+1}(x_{nm})} J_n\left(x_{nm} \frac{\rho}{R}\right) e^{in\phi}, \quad (45)$$

where  $x_{nm}$  is the  $m$ th root of the equation  $J_n(x) = 0$ . The spectrum is given by equation (44) with  $y_{nm}$  replaced by  $x_{nm}$  and  $n_z \geq 0$ .

Denoting the modes by  $(n, m, n_z)$ , the lowest TE mode is (1, 1, 1), and it has a frequency  $\omega_{111} = (1.841/R)\sqrt{1 + 2.912(R/L_z)^2}$ . This mode is uncoupled to any other modes, and according to equation (38) the number of photons in this mode grows exponentially in time as  $\exp(\pi\epsilon t/\sqrt{1 + 0.343(L_z/R)^2 L_z})$  when parametrically excited. It is interesting to point out that for this mode it is possible to tune the resonance by changing the relation of the radius and the height of the cavity. The lowest TM mode (0, 1, 0) is also uncoupled, and it has a frequency  $\omega_{010} = 2.405/R$ . From equation (39) we find the parametric growth to be  $\exp(4.81\epsilon t/R)$ . This mode cannot be resonated by simple tuning since its frequency depends solely on the radius of the cylinder. For  $L_z$  large enough ( $L_z > 2.03R$ ), the resonance frequency  $\omega_{111}$  of the lowest TE mode is smaller than that for the lowest TM mode. Then the (1, 1, 1) TE mode is the fundamental oscillation of the cavity.

**Table 1.** Values of  $\frac{2\lambda}{\omega}$  for different cavities. In the cubic case, the values are independent of the size  $L$ . For cylindrical cavities of length  $L$  and circular section of radius  $R$ , we are assuming  $L/R = 10$ .

Cavity	Mode	$2\lambda/\omega$
Cubic	TE (1, 0, 1)	0.5
Cubic	TE (0, 1, 1)	0.5
Cubic	TM (1, 1, 0)	1.0
Cubic	TM (1, 1, 4)	0.3
Cylindrical	TM (0, 1, 0)	2.0
Cylindrical	TE (1, 1, 1)	0.03

### 4.3. Numerical estimations

The number of generated photons computed in the previous sections is in general proportional to  $\exp[2\lambda\epsilon t]$ , where  $\lambda$  depends on the geometry and the particular mode considered (see for example equations (38) and (39), that are valid for uncoupled modes). The amount of created photons is limited by the  $Q$  factor of the cavity. If the mirror oscillates during a time  $t_{\max} \simeq Q/\omega$  (with  $\omega$  the frequency of the mode), the maximum number of particles is  $\exp[\frac{2\lambda}{\omega}\epsilon Q]$ . In table 1 we show the value of  $\frac{2\lambda}{\omega}$  for the lowest modes in cavities with rectangular and circular sections. The maximal dimensionless amplitude for the mechanical oscillation of the mirror is of order  $\epsilon_{\max} \simeq 10^{-8}$  [5]. Therefore, a very high  $Q$  factor is needed to produce a large number of photons.

The constraint over  $Q$  can be relaxed if, instead of considering moving mirrors, one considers a cavity containing a thin semiconductor film. The effective length of the cavity can be changed by irradiating the semiconductor [12–15]. In this situation, the maximum number of created photons is of order  $\exp[a\tilde{\epsilon}Q]$ , where  $a = O(1)$  and  $\tilde{\epsilon}$  depends on the properties of the semiconductor and on the geometry of the cavity. For reasonable values of the parameters one can have values of  $\tilde{\epsilon}$  as large as  $\simeq 10^{-2}$  [15]. In this case, a large number of photons can be produced, even if the  $Q$  factor is not so high. For example, for conservative values  $Q = 10^6$ ,  $\tilde{\epsilon} = 10^{-4}$ ,  $a = 1$  the number of created photons is of order  $10^{43}$ .

## 5. Non-simply connected cavities: transverse electromagnetic modes

When the cylindrical cavity is non-simply connected, in addition to the TE and TM modes one should also consider the TEM modes, for which both the electric and magnetic fields have vanishing  $z$  components. The treatment of the TE and TM modes in these cavities is similar to the case of hollow cylinders. However, to describe the TEM modes it is necessary to introduce an additional scalar field  $\varphi(z, t)$ . Indeed, working with the usual vector potential  $\mathbf{A}$ , the TEM solutions are of the form

$$\mathbf{A}(\mathbf{x}_{\perp}, z, t) = \mathbf{A}_{\perp}(\mathbf{x}_{\perp})\varphi(z, t), \quad (46)$$

$$\mathbf{E} = -(\partial_t\varphi) \mathbf{A}_{\perp}, \quad (47)$$

$$\mathbf{B} = (\partial_z\varphi) \hat{\mathbf{z}} \times \mathbf{A}_{\perp}. \quad (48)$$

The transverse vector potential has vanishing rotor and divergence, and zero tangential component on the transverse surfaces. Therefore,  $\mathbf{A}_{\perp}$  is a solution of an

*electrostatic* problem in the two transverse dimensions (in hollow cylindrical cavities the transverse potential vanishes and TEM modes do not exist). The scalar field  $\varphi$  satisfies Dirichlet boundary conditions on the longitudinal boundaries  $z = 0$  and  $z = L_z(t)$ , and the longitudinal wave equation  $(\partial_t^2 - \partial_z^2)\varphi = 0$ . For a static cavity, the eigenfrequencies of the TEM modes are  $w_n = n\pi/L_z$ . Note that this is an equidistant spectrum. In the particular case of a resonant cavity formed with two concentric cylinders, the transverse vector potential is given by  $\mathbf{A}_{\perp} = \hat{\rho}/\rho$ . However, it is important to stress that the description in this section is valid for a non-simply connected cavity of arbitrary section.

In order to quantize these TEM modes, we proceed as in section 3. The Hamiltonian associated with TEM modes is

$$\begin{aligned} H^{\text{TEM}} &= \frac{1}{8\pi} \int d^2x_{\perp} dz (\mathbf{E}^2 + \mathbf{B}^2) \\ &= \frac{1}{8\pi} \left( \int d^2x_{\perp} |\mathbf{A}_{\perp}|^2 \right) \int dz [(\partial_t\varphi)^2 + (\partial_z\varphi)^2]. \end{aligned} \quad (49)$$

The above equation shows that the quantization of TEM modes is equivalent to the quantization of a scalar field in  $1 + 1$  dimensions with Dirichlet boundary conditions at  $z = 0$  and  $z = L_z(t)$ . This problem has been previously studied as a toy model for the dynamical Casimir effect [3]. It is interesting that this toy model describes TEM waves in non-simply connected cavities.

Due to the conformal symmetry, in  $1 + 1$  dimensions it is possible to write down an explicit expression for the modes in terms of a single function satisfying the so-called Moore equation [21]. This equation can be solved, for example, using a renormalization group improvement of the perturbative solution [22]. We will not repeat the analysis here, but just quote the main results. As the eigenfrequencies are equidistant, there is intermode coupling, and the spectrum of created photons is completely different from the  $3 + 1$  case. If the external frequency is  $\Omega = q\pi/L_z$  with  $q$  an integer,  $q \geq 2$ , photons are created resonantly in all modes with  $n = q + 2j$ , with  $j$  being a non-negative integer. The number of photons in each mode does not grow exponentially, but the total energy inside the cavity does.

Using the conformal symmetry in  $1 + 1$  dimensions, it is possible to compute not only the total energy inside the cavity but also the mean value of the energy density:

$$\begin{aligned} \langle T_{00}^{\text{TEM}}(\mathbf{x}, t) \rangle &= \frac{1}{8\pi} |\mathbf{A}_{\perp}|^2 [(\partial_t\varphi)^2 + (\partial_z\varphi)^2] \\ &\equiv \frac{1}{4\pi} |\mathbf{A}_{\perp}(\mathbf{x}_{\perp})|^2 \langle T_{00}(z, t) \rangle. \end{aligned} \quad (50)$$

It can be shown that the one-dimensional energy density  $\langle T_{00}(z, t) \rangle$  grows exponentially in the form of  $q$  travelling wavepackets which become narrower and higher as time increases. As an example, in figure 2 we show the energy density profile as a function of  $z$  for a fixed  $t$  and for the case  $q = 4$ . As time evolves, the peaks move back and forth, bouncing against the caps of the cavity. The height of the peaks increases as  $\exp(\frac{2\pi q\epsilon t}{L_z})$  and their width decreases as  $\exp(-\frac{\pi q\epsilon t}{L_z})$ , so that the total area beneath each peak, and hence the total energy inside the cavity, grows as  $\exp(\frac{\pi q\epsilon t}{L_z})$ . In figure 3 the energy density is shown as a function of time at the mid-point  $z = L_z/2$ , also for the  $q = 4$  case. This is proportional to the signal that should be measured by a detector placed at that point.

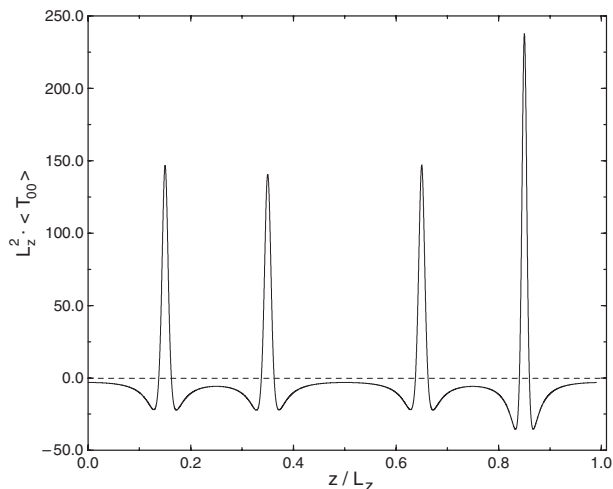


**Figure 2.** One-dimensional energy density profile  $\langle T_{00}(z, t) \rangle$  for fixed time  $t/L_z = 20.4$  for the  $q = 4$  case. The amplitude coefficient is  $\epsilon = 0.01$ .

## 6. Conclusions

In this paper we have analysed the non-stationary Casimir effect for cylindrical cavities with arbitrary section and time-dependent length. Using Hertz potentials, we have shown that for hollow cylinders the full electromagnetic problem can be treated by considering two scalar fields, one satisfying Dirichlet boundary conditions and the other generalized Neumann boundary conditions on the caps of the cavity. We have derived explicit formulae for the number of TE and TM photons created during the motion of the mirror in terms of the Bogoliubov transformation connecting the IN and OUT bases of the scalar fields. We have also shown the equivalence between the Hertz potential approach and the dual vector potentials approach used in previous papers.

Using the TE and TM scalar fields, we rederived results for the number of photons created in resonant situations for cavities of rectangular section, and we computed the TE and TM photon creation in cavities with circular section.

We also considered non-simply connected cylindrical cavities. In this case, it is necessary to introduce a third scalar field satisfying Dirichlet boundary conditions to take into account the TEM waves. We have shown that the dynamics of this field is equivalent to that of a scalar field in 1 + 1 dimensions. Therefore, all results derived previously in ‘toy models’ are useful to describe the creation of TEM photons, i.e., TEM modes provide a realistic realization of the models in 1+1 dimensions. This is interesting not only from a theoretical point of view. Indeed, TEM modes have in general a lower fundamental frequency than TE and TM modes (this is the case for example for a rectangular cavity containing an inner cylinder along the longest direction). This is important, since one of the main difficulties in measuring the dynamical Casimir effect is to produce oscillations of the mirror at twice the lowest frequency of the cavity. Moreover, as the eigenfrequencies of TEM modes are equidistant, the modes are coupled and the energy density in the cavity develops a very particular structure that might be detected more easily than photons of a given frequency. Taking into account these results, it may

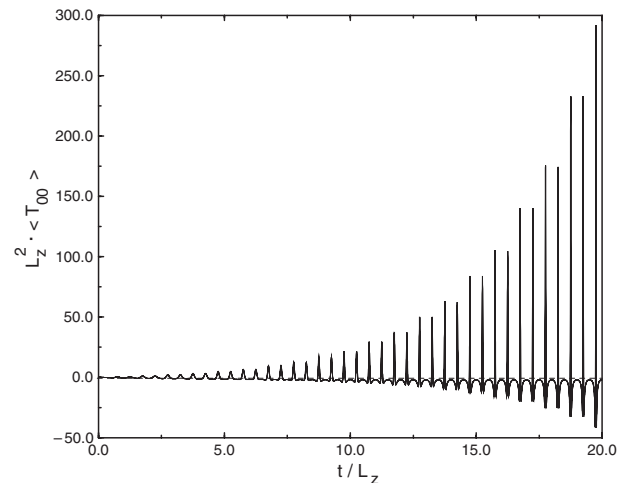


**Figure 3.** One-dimensional energy density profile  $\langle T_{00}(z, t) \rangle$  for the midpoint  $z/L_z = 0.5$  between the caps of the cavity. The parameters are  $q = 4$  and  $\epsilon = 0.01$ .

be of interest to excite TEM photons by changing the effective length of a cavity by irradiating a semiconductor placed inside it. This could be done by inserting a metallic cylinder into the cavities used in the experiments of [14].

## Acknowledgments

FCL and FDM were supported by Universidad de Buenos Aires, CONICET, Fundación Antorchas and Agencia Nacional de Promoción Científica y Tecnológica, Argentina. MC and DARD thank Carlos Villarreal for useful conversations on Hertz potentials. We would like to thank the organizers of this topical issue, Gabriel Barton, Victor V Dodonov and Vladimir I Man’ko, for the invitation to submit a paper.

## References

- [1] Birrell N D and Davies P C D 1982 *Quantum Fields in Curved Space* (London: Cambridge University Press)
- [2] Dodonov V V 2001 *Adv. Chem. Phys.* **119** 309
- [3] Law C K 1991 *Phys. Rev. Lett.* **73** 1931  
Law C K and Shieve W C 1995 *Phys. Rev. A* **52** 4405  
Dodonov V V, Klimov A B and Man’ko V I 1990 *Phys. Lett. A* **149** 225  
Lambrecht A, Jaekel M-T and Reynaud S 1996 *Phys. Rev. Lett.* **77** 615  
Lambrecht A, Jaekel M-T and Reynaud S 1998 *Europhys. Lett.* **43** 147  
Dalvit D A R and Mazzitelli F D 1998 *Phys. Rev. A* **57** 2113  
Dalvit D A R and Mazzitelli F D 1999 *Phys. Rev. A* **59** 3049
- [4] Croce M, Dalvit D A R and Mazzitelli F D 2001 *Phys. Rev. A* **64** 013808
- [5] Dodonov V V and Klimov A B 1996 *Phys. Rev. A* **53** 2664
- [6] Croce M, Dalvit D A R and Mazzitelli F D 2002 *Phys. Rev. A* **66** 033811
- [7] Dodonov A V, Dodonov E V and Dodonov V V 2003 *Phys. Lett. A* **317** 378
- [8] Plunien G, Schützhold R and Soff G 2000 *Phys. Rev. Lett.* **84** 1882
- [9] Bordag M, Mohideen U and Mostepanenko V M 2001 *Phys. Rep.* **353** 1
- [10] Lamoreaux S K 1997 *Phys. Rev. Lett.* **78** 5  
Mohideen U and Roy A 1998 *Phys. Rev. Lett.* **81** 4549  
Chan H B et al 2001 *Science* **291** 1941  
Bressi G et al 2002 *Phys. Rev. Lett.* **88** 041804

- Decca R S *et al* 2003 *Phys. Rev. Lett.* **91** 050402
- [11] Onofrio R 2004 *Quantum Field Theory Under the Influence of External Conditions* ed K A Milton (Princeton, NJ: Rinton Press)
- [12] Lozovik Y E, Tsvetus V G and Vinogradov E A 1995 *Phys. Scr.* **52** 184  
Lozovik Y E, Tsvetus V G and Vinogradov E A 1995 *JETP Lett.* **61** 723
- [13] Yablonovitch E 1989 *Phys. Rev. Lett.* **62** 1742
- [14] Carugno G *et al* 2002 *MIR Project* unpublished  
Braggio C *et al* 2004 *Rev. Sci. Instrum.* **75** 49676 (*Preprint quant-ph/0411085*)
- [15] Croce M, Dalvit D A R, Lombardo F C and Mazzitelli F D 2004 *Phys. Rev. A* **70** 033811
- [16] Nisbet A 1955 *Proc. R. Soc. A* **231** 250
- [17] Hacyan S, Jáuregui R, Soto F and Villarreal C 1990 *J. Phys. A: Math. Gen.* **23** 2401
- [18] Jackson J D 1998 *Classical Electrodynamics* 3rd edn (New York: Wiley)
- [19] Maia Neto P A 1994 *J. Phys. A: Math. Gen.* **27** 2164  
Mundarain D F and Maia Neto P A 1998 *Phys. Rev. A* **57** 1379
- [20] Namias V 1988 *Am. J. Phys.* **56** 898
- [21] Moore G T 1970 *J. Math. Phys.* **11** 2679
- [22] See, Dalvit D A R and Mazzitelli F D in [3]